MOEM

Modern Electronic Materials 2024; 10(2): 85–90
DOI 10.3897/j.moem.10.2.129762

Research Article

Optically transparent highly conductive contact based on ITO and copper metallization for solar cells

Vladimir M. Kravchenko[1], Victoria V. Malyutina-Bronskaya[1], Hanna S. Kuzmitskaya[1], Anton V. Nestsiaronak[1]

1 State Scientific and Production Association of Optics, Optoelectronics and Laser Technology, 68-1 Nezavisimosti Ave., Minsk 220072, Republic of Belarus

Corresponding author: Victoria V. Malyutina-Bronskaya (malyutina@oelt.basnet.by)

Received 15 May 2024 ♦ **Accepted** 21 June 2024 ♦ **Published** 2 July 2024

Citation: KravchenkoVM, Malyutina-Bronskaya VV, Kuzmitskaya HS, NestsiaronakAV (2024) Optically transparent highly conductive contact based on ITO and copper metallization for solar cells. *Modern Electronic Materials* 10(2): 85–90. https://doi.org/10.3897/j.moem.10.2.129762

Abstract

This paper presents the results of obtaining and studying the electrical and optical characteristics of an optically transparent highly conductive Ni/Cu/Ti/ITO contact in order to reduce electrical resistance losses on the front side of the silicon solar cell. The topology of the contact metallization is a square 50 × 50 mm^2 with an interdigitated electrode structure. A Ni/Cu/Ti contact metallization formed on ITO layer reduces the surface resistance by more than 60 times. It has been shown that the use of a Ni/Cu/Ti contact with a finger thickness of at least 1.5 μm and a width of 17 μm was formed is a good alternative to traditional contacts for silicon solar cells based on silver paste.

Keywords

ITO, copper metallization, solar elements, contact resistivity

1. Introduction

Optical and ohmic losses are the main reasons for reducing the efficiency of a solar cell (SC). The metallization of the front side of the solar cell is responsible for collecting, transporting and transferring currents. The geometry and material of the front metallization affects the operating efficiency and parameters of solar cells [1–6].

Screen printing is the leading electrode deposition technology in mass production of photovoltaic systems due to its simplicity and high productivity. However, the resistivity of low temperature silver paste results in increased contact resistance and shading loss of finger width, which limits the cell performance [7]. Copper metallization of the silicon SC is a competitive alternative. The resistivity of the copper electrode is close to the bulk copper material, which is 2 to 3 times lower than that of the printed silver electrode, and can achieve a reduction in contact resistance [8]. The main materials for contact metallization of solar cells are: nickel (Ni), silver (Ag), copper (Cu) [9].

Table 1 shows a comparison of the parameters and costs of Cu, Ag and Ni. It can be seen that the resistivity of copper is only 3.7% higher compared to silver, and the cost is about 100 times less, which is an important factor in reducing costs, since the use of silver accounts for 10% of the cost of a typical solar module [8, 10].

One of the current developments in copper plating is the electroplating method using a sacrificial organic resistive mask on a transparent conductive oxide (TCO).

Table 1. Comparison of parameters and costs of materials for metallization [8, 10]

Parameter	Materials		
	Ag	Cu	Ni
Conductivity (10^6 S/m)	61.4	59.1	13.9
Density (g/cm^3)	10.5	8.9	8.9
Cost (USD/kg)	808.0	8.0	24.0

Using this technology, developers have achieved the silicon heterojunctions (SHJ) SC efficiency of about 25% [7, 11].

Considering alternative metals for SC front plating, many researchers have demonstrated that the use of Ni/Cu-based plating for SC results in the improved fill factor (FF) and efficiency compared to conventional silver-plated SC [12, 13]. Ni/Cu-based metallization offers potential benefits for SC in the form of narrower finger lines, lower series resistance, and lower material costs. The main disadvantage of Cu is its relatively high mobility and the fact that it is a highly efficient recombination center in silicon [14, 15]. This requires a diffusion barrier such as Ni to prevent Cu from diffusion into silicon. The nickel silicide formed at the interface reduces the contact resistance, which will ensure minimal power loss due to series resistance (R_S) in the SC. Sun Power Corporation (USA) proposed SC with interdigitated back contacts based on Al, followed by Ni–Cu–Ag coating with additional annealing, which made it possible to obtain a SC with a record efficiency of 24% [16, 17].

It can be noted that the ITO layer used as a transparent conductive contact, which also provides an effective barrier against copper diffusion [18–20]. Works [4, 7] consider the electrical properties of Mo/Al/ITO, Ti/Al/ITO, Cr/Ni/Al/ITO, Cu_xNi_{1-x}/ITO systems as alternative screen-printing materials for obtaining metallized transparent conductive contacts to SCs.

It is important to note that when developing the topology of SC contact metallization, it is necessary to take into account the fact that metal contact bars play an important role in contributing to the overall power losses of the SC. Losses lower as the finger resistance decreases. With low resistance of contact metallization, first of all, losses depend on the geometric parameters of the buses (height and width), and only then optical losses associated with the width of the fingers begin to work [21]. Therefore, an important task is to match the optical shading from metal busbars and the loss of electrical resistance on the front side of the SC. A significant reduction in finger width from 72 to 15 μm is observed between silver paste screen-printing and copper electroplating methods. Based on the measured geometric characteristics of the fingers for the two methods described above, losses associated with optical shading by fingers of 5.3% (screen-printing) and 2.1% (electrodeposition), respectively, were obtained, which led to theoretical gain in current J_c of 1.3 mA/cm^2 when using galvanic deposition of copper [22].

Thus, the goal of the work was to obtain and investigate the properties of contact metallization Ni/Cu/Ti of optically transparent high-conductivity contacts based on ITO.

2. Experimental

The formation of an optically transparent film (ITO) on the K8 glass substrate with a diameter of d = 76 mm was carried out using the electron beam deposition method in a vacuum. This method ensures high quality of deposited thin films while controlling their thickness with good reproducibility of parameters. The starting material for evaporation was tablets of the compound In_2O_3 and SnO_2 in a ratio of 9 : 1 (ITO), consisting of indium oxide 90 wt.% and tin oxide 10 wt.%, purity 99.99%. The pressure of the residual gases in the deposition chamber was $6 \cdot 10^{-4}$ Pa; during deposition, pure gaseous oxygen (99.99%) was introduced to a pressure of $6 \cdot 10^{-2}$ Pa. The substrate temperature has been maintained at 350 °C during the deposition process.

The thickness of thin films during the deposition process was carried out using a spectrometer built into a vacuum chamber, which operated in the transmission mode. Such control makes it possible to form high-quality thin films with a thickness of 40 nm or more of various materials with an accuracy of 1 nm and it increases the reproducibility of results. Additionally, to control the deposition rate and thickness of thin films, quartz microbalances, also located in a vacuum chamber, are used [23, 24]. In this way, the thickness of the deposited ITO film has been determined as 0.23 μm.

The optically transparent ITO film was deposited with Ti/Cu/Ni metallization using electron beam sputtering. The starting material for the evaporation of metals was Ti, Cu, Ni granules of 99.95% purity. The Ti layer was deposited to ensure good adhesion when Cu was deposited onto an optically transparent electrically conductive contact, and the Ni layer was deposited to protect Cu from the oxidative processes of the surrounding atmosphere.

The structure for contact metallization of optically transparent conductive contacts was developed for applying contact metallization to round plates with a diameter of 76 mm, on the basis of which the topology of the photomask was implemented. The topology of the photomask is a square 50 × 50 mm^2 in size with an interdigitated electrode structure. Two main collecting bars measuring 50 × 1.5 mm^2 have a square protrusion for unsoldering electrodes measuring 2 × 2 mm^2. Finger size: width 50 μm, length 49.25 mm. The gap between the fingers and the gap between the collecting busbar and the end of the finger are 750 μm. The manufactured photomask, the appearance of which is shown in Fig. 1*a*, is a plate of borosilicate glass with dimension 127 × 127 mm^2 and thickness 2.6 ± 0.3 mm with a chrome coating.

Using positive photolithography and a developed photomask, a pattern of Ti/Cu/Ni contact metallization with

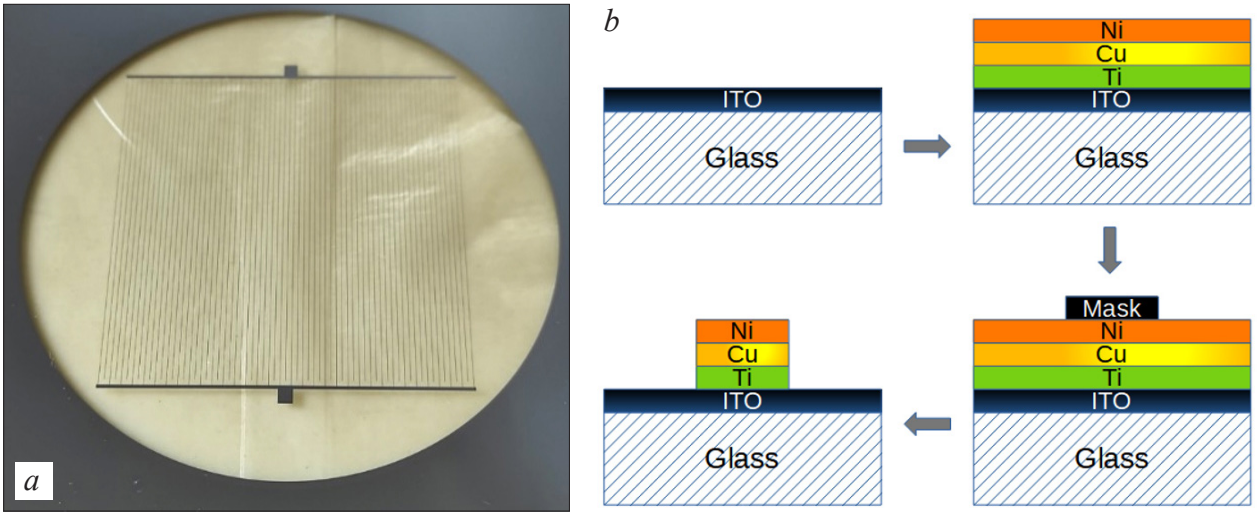

Figure 1. Photograph of the photomask (*a*) and the sequence of formation of metallized wiring on the ITO/glass structure using photolithography (*b*)

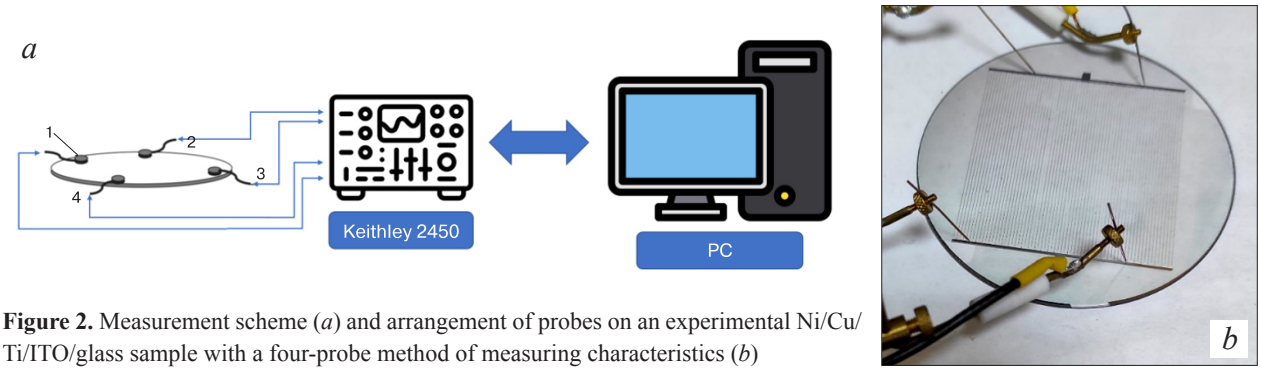

Figure 2. Measurement scheme (*a*) and arrangement of probes on an experimental Ni/Cu/Ti/ITO/glass sample with a four-probe method of measuring characteristics (*b*)

an interdigitated electrode structure with a thickness of at least 1.5 μm and a width of 17 μm was formed. The scheme for obtaining a metallization pattern on optically transparent electrically conductive materials using photolithography is shown in Fig. 1*b*.

Optical control was carried out using an MBS-9 optical microscope and a Levenhuk M1600 Plus digital camera.

Analysis of the transmission spectra of the optically transparent conductive ITO coating on glass in the wavelength range from 300 to 1100 nm with a step of 0.25 nm was performed on a PHOTON RT spectrophotometer (Belarus).

Resistance measurements were carried out on Keithley 2450 meter and the resistance of experimental samples of contact metallization was measured using the 4-probe method. Fig. 2 shows the measurement scheme (Fig. 2*a*) and the location of the probes on the experimental sample (Fig. 2*b*).

3. Results and discussion

The transmission spectrum was measured on the ITO/glass structure, which showed that the ITO film has an optical band gap of 3.67 eV and a transmittance in the wavelength range λ = 450−1100 nm on average greater than 80% (Fig. 3). The transmission spectra have an oscillating character, due to interference phenomena in the film–substrate system. The resistance of the ITO layer, measured by the 4-probe method, was 25 Ohm/□.

The appearance of the experimental sample of the Ni/Cu/Ti/ITO/glass structure is shown in Fig. 4*a*. As a result, the required metallization pattern with good adhesion

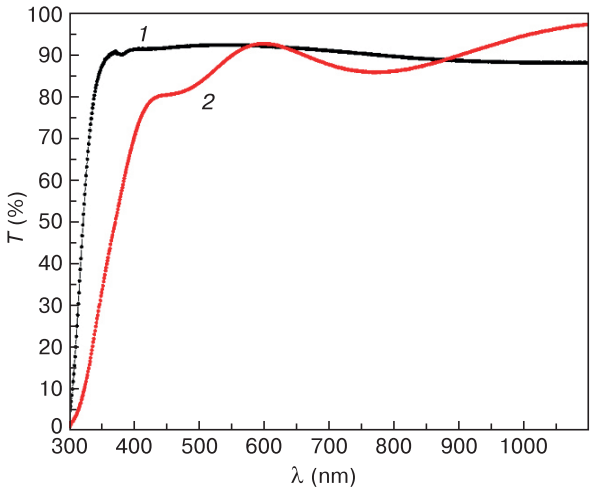

Figure 3. Transmission spectrum of K8 glass (*1*) and ITO film on glass (*2*)

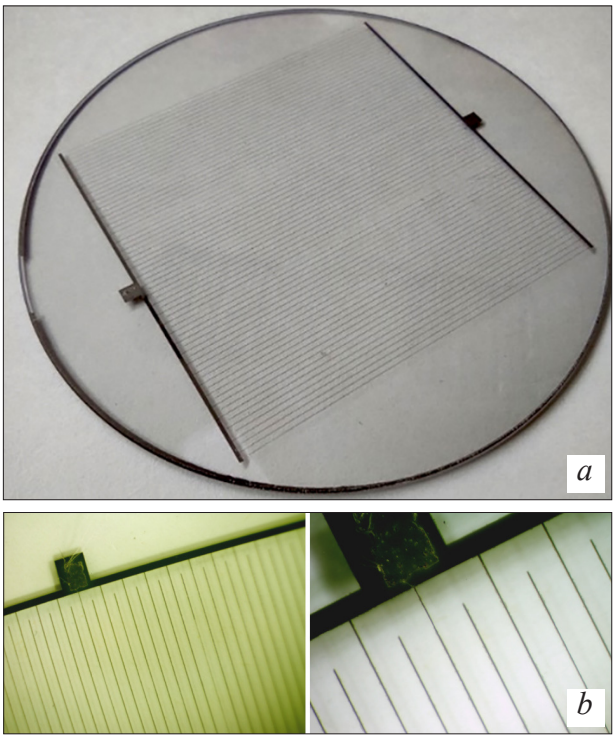

Figure 4. Photograph of the experimental sample of the Ni/Cu/Ti/ITO/glass structure (*a*) and optical microscopy images of the metallized Ti/Cu/Ni wiring with magnification (*b*)

was formed on the ITO surface, as shown by optical control (Fig. 4*b*).

Additionally, it was taken into account that the ITO layer acts as an antireflection coating for maximum input of incident radiation. In this case, condition (1) should be realized [22]:

$$n^2(\text{ITO}) = n(\text{air}) \cdot n(\text{Si}), \quad (1)$$

where n is refractive index of material.

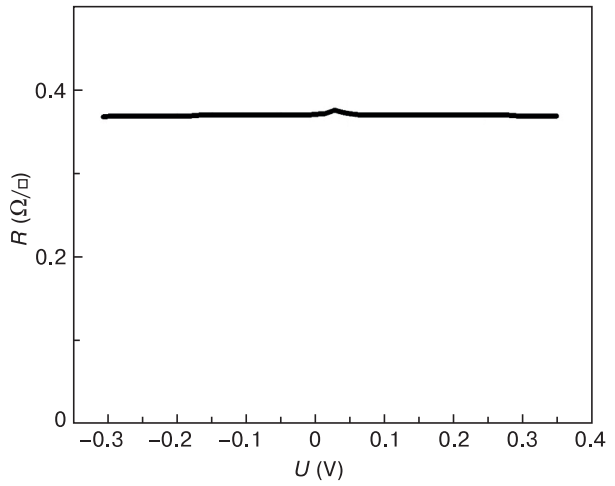

Figure 5. Resistance of the experimental sample of the Ni/Cu/Ti/ITO/glass structure

In our case we have: n(air) = 1, n(Si) = 3.44, n(ITO) = 1.80 [25–27]. Thus, we obtain a minimum mismatch for this parameter, which will ultimately ensure an input of more than 80%, and when using an additional antireflective coating MgF_2 (n = 1.38) [22, 28] on top of Ni/Cu/Ti/ITO metallization, more than 90% of the falling radiation in the visible range. And the area of metallization deposited on the ITO layer will result in shading losses of less than 3%.

Fig. 5 shows typical resistance measurement results for experimental samples of the Ni/Cu/Ti/ITO/glass structure. The resistance of the experimental sample was 0.37 Ohm/□.

The total resistance R_{total} of the metal/ITO contact system is:

$$R_{\text{total}} = 2R_c + 2R_M + R_{\text{ITO}}, \quad (2)$$

where R_c is the contact resistance between the metal and ITO, R_M is the metal resistance, which can be neglected, and R_{ITO} is ITO resistance. If the distance between the metal fingers is very small, we can approximate $R_{\text{total}} \rightarrow 2R_c$; now we can calculate R_c [29].

Considering that the thickness of the deposited ITO film was 0.23 μm, and the width of the metallization was 5 cm, the effective area of current flow is $1.15 \cdot 10^{-4}$ cm^2. Taking into account the Eq. (1) and the resulting effective area of current flow, we obtain a contact resistance of the order of $0.43 \cdot 10^{-4}$ Ω·cm^2. The obtained value of contact resistance turned out to be an order of magnitude lower than for different ITO/metal systems used as contact metallization of SC: ITO/Mo/Al – $1.8 \cdot 10^{-2}$ Ω·cm^2, ITO/Ti/Al – $8.7 \cdot 10^{-3}$ Ω·cm^2, ITO/Cr/Ni/Al – $8.1 \cdot 10^{-2}$ Ω·cm^2; ITO/CuNi – $1.2 \cdot 10^{-3}$ Ω·cm^2 [30, 31].

4. Conclusions

In this work, the properties of an optically transparent highly conductive contact based on the Ni/Cu/Ti/ITO/glass structure were investigated. The ITO film had a transmittance in the wavelength range λ from 450 to 1100 nm on average greater than 80%. The resistance of the ITO layer, measured by the 4-probe technique, was 25 Ohm/□.

A Ni/Cu/Ti contact metallization formed on ITO in the shape of a square measuring 50 × 50 mm^2 with an interdigitated electrode structure no less than 1.5 μm thick and 17 μm wide made it possible to obtain an optically transparent contact resistance of about 0.37 Ohm/□. Taking into account the effective area of current flow, its contact resistance was estimated, which amounted to $0.43 \cdot 10^{-4}$ Ω·cm^2. The results obtained show that optically transparent highly conductive contacts based on the Ni/Cu/Ti/ITO structure are promising for optoelectronic devices, including increasing the operating efficiency of silicon solar cells by reducing electrical losses.

References

1. Li L., Tu J.L., Yang Y., Wu J., Hu K., Yu S. Effect of finger interruption mode on the performance of crystalline silicon solar cells. *Solar Energy*. 2022; 238: 381–391. https://doi.org/10.1016/j.solener.2022.03.065
2. Drabczyk K., Panek P. Influence of screen-printing parameters on the front metallic electrodes geometry of solar cells. *Circuit World*. 2014; 40(1): 23–26. https://doi.org/10.1108/CW-10-2013-0038
3. Magnone P., Napoletano G., De Rose R., Crupi F., Tonini D., Cellere G., Galiazzo M., Sangiorgi E., Fiegna C. A methodology to account for the finger non-uniformity in photovoltaic solar cell. *Energy Procedia*. 2012; 27: 191–196. https://doi.org/10.1016/j.egypro.2012.07.050
4. Lee S.H., Lee D.W., Lim K., Shin W., Kim J. Copper-nickel alloy plating to improve the contact resistivity of metal grid on silicon heterojunction solar cells. *Electronic Materials Letters*. 2019; 15: 314–322. https://doi.org/10.1007/s13391-019-00134-x
5. Raval M.C., Solanki C.S. Review of Ni-Cu based front side metallization for c-Si solar cells. *Journal of Solar Energy*. 2013: 183812. http://dx.doi.org/10.1155/2013/183812
6. Lennon A., Yao Y., Wenham S. Evolution of metal plating for silicon solar cell metallisation. *Progress in Photovoltaics*. 2013; 21(7): 1454–1468. https://doi.org/10.1002/pip.2221
7. Yu J., Li J., Zhao Y., Lambertz A., Chen T., Duan W., Liu W., Yang X., Huang Y., Ding K. Copper metallization of electrodes for silicon heterojunction solar cells: Process, reliability and challenges. *Solar Energy Materials and Solar Cells*. 2021; 224: 110993. https://doi.org/10.1016/j.solmat.2021.110993
8. Schuster C.E., Vangel M.G., Schafft H.A. Improved estimation of the resistivity of pure copper and electrical determination of thin copper film dimensions. *Microelectronics Reliability*. 2001; 41(2): 239–252. https://doi.org/10.1016/S0026-2714(00)00227-4
9. Rehman A.U, Lee S.H. Review of the potential of the Ni/Cu plating technique for crystalline silicon solar cells. *Materials* 2014; 7(2): 1318–1341. https://doi.org/10.3390/ma7021318
10. Unsur V. Implementation of nickel and copper as cost-effective alternative contacts in silicon solar cells. *Progress in Photovoltaics*. 2024; 32(4): 267–275. https://doi.org/10.1002/pip.3792
11. Hernández J.L., Adachi D., Schroos D., Valckx N., Menou N., Uto T., Hino M., Kanematsu M., Kawasaki H., Mishima R., Nakano K., Uzu H., Terashita T., Yoshikawa K., Kuchiyama T., Hiraishi M., Nakanishi N., Yoshimi M., Yamamoto K. High efficiency copper electroplated heterojunction solar cells and modules – the path towards 25% cell efficiency. *In: Proc. 28th Eur. Photovoltaic Solar Energy Conf. Exhib.*; 2013: 247–250. https://doi.org/10.4229/28thEUPVSEC2013-2AO.2.1
12. Lee E.J., Kim D.S., Lee, S.H. Ni/Cu metallization for low-cost high-efficiency PERC cells. *Solar Energy Materials and Solar Cells*. 2002; 74(1–4): 65–70. https://doi.org/10.1016/S0927-0248(02)00049-1
13. Kim D.S., Lee E.J., Kim J., Lee S.H. Low-cost contact formation of high-efficiency crystalline silicon solar cells by plating. *Journal of the Korean Physical Society*. 2005; 46: 1208–1212.
14. Dolbak A.E., Zhachuk R.A., Olshanetsky B.Z. Mechanism of copper diffusion over the Si (110) surface. *Semiconductors*. 2002; 36: 958–961. https://doi.org/10.1134/1.1507271
15. Kraft A., Wolf C., Bartsch J., Glatthaar M. Characterization of copper diffusion in silicon solar cells. *Energy Procedia*. 2015; 67: 93–100. https://doi.org/10.1016/j.egypro.2015.03.292
16. Wilson G.M., Al-Jassim M., Metzger W.K., Glunz S.W., Verlinden P., Xiong G., Mansfield L.M., Stanbery B.J., Zhu K., Yan Y., Berry J.J., Ptak A.J., Dimroth F., Kayes B.M., Tamboli A.C., Peibst R., Catchpole K., Reese M.O., Klinga C.S., Denholm P., Morjaria M., Deceglie M.G., Freeman J.M., Mikofski M.A., Jordan D.C., TamizhMani G., Sulas-Kern D.B. The 2020 photovoltaic technologies roadmap. *Journal of Physics D: Applied Physics*. 2020; 53(49): 493001. https://doi.org/10.1088/1361-6463/ab9c6a
17. Adachi D., Hernández J.L., Yamamoto K. Impact of carrier recombination on fill factor for large area heterojunction crystalline silicon solar cell with 25.1% efficiency. *Applied Physics Letters*. 2015; 107: 233506. https://doi.org/10.1063/1.4937224
18. Liu C.M., Liu W.L., Chen W.J., Hsieh S.H., Tsai T.K., Yang L.C. ITO as a diffusion barrier between Si and Cu. *Journal of the Electrochemical Society*. 2005; 152(3): 234–239. https://doi.org/10.1149/1.1860511
19. Hsieh S.H., Chien C.M., Liu W.L., Chen W.J. Failure behavior of ITO diffusion barrier between electroplating Cu and Si substrate annealed in a low vacuum. *Applied Surface Science*. 2009; 255(16): 7357–7360. https://doi.org/10.1016/j.apsusc.2009.04.001
20. Hsieh S.H., Chen W.J., Ohdaira K. Barrier performance of ITO film on textured Si substrate. *Journal of Materials Science: Materials in Electronics*. 2020; 31: 13808–13816. https://doi.org/10.1007/s10854-020-03941-3
21. Yu J., Bian J., Duan W., Liu Y., Shi J., Meng F., Liu Z. Tungsten doped indium oxide film: Ready for bifacial copper metallization of silicon heterojunction solar cell. *Solar Energy Materials and Solar Cells*, 2016; 144: 359–363. https://doi.org/10.1016/j.solmat.2015.09.033
22. Geissbühler J., de Wolf S., Faes A., Badel N., Jeangros Q., Tomasi A., Barraud L., Descoeudres A., Despeisse M., Ballif C. Silicon heterojunction solar cells with copper-plated grid electrodes: status and comparison with silver thick-film techniques. *IEEE Journal of Photovoltaics*. 2014; 4(1): 1055–1062. https://doi.org/10.1109/JPHOTOV.2014.2321663
23. Lu C.-S., Lewis O. Investigation of film-thickness determination by oscillating quartz resonators with large mass load. *Journal of Applied Physics*. 1972; 43(11): 4385–4390. https://doi.org/10.1063/1.1660931
24. Mecea V.M. Is quartz crystal microbalance really a mass sensor? *Sensors and Actuators A: Physical*. 2006; 128(2): 270–277. https://doi.org/10.1016/j.sna.2006.01.023
25. Ciddor P.E. Refractive index of air: new equations for the visible and near infrared. *Applied Optics*. 1996; 35(9): 1566–1573. https://doi.org/10.1364/AO.35.001566
26. Chandler-Horowitz D., Amirtharaj P.M. High-accuracy, midinfrared (450 $cm^{-1} \leq \omega \leq 4000\ cm^{-1}$) refractive index values of silicon. *Journal of Applied Physics*. 2005; 97(12): 123526. https://doi.org/10.1063/1.1923612
27. Minenkov A., Hollweger S., Duchoslav J., Erdene-Ochir O., Weise M., Ermilova E., Hertwig A., Schiek M. Monitoring the electrochemical failure of indium tin oxide electrodes via operando

ellipsometry complemented by electron microscopy and spectroscopy. *ACS Applied Materials & Interfaces*. 2024; 16(7): 9517–9531. https://doi.org/10.1021/acsami.3c17923

28. Zhao C., Chao M.A., Liu J., Liu Z., Chen Y. Sputtering power on the microstructure and properties of MgF_2 thin films prepared with magnetron sputtering. *Journal of Inorganic Materials*. 2020; 35(9): 1064–1070. https://www.researching.cn/ArticlePdf/m00097/2020/35/9/1064.pdf
29. Zhao Y. Design and analysis of antireflection layer on the surface of crystalline silicon solar cell. *Bulletin of Science and Practice*. 2022; 8(6): 470–491. https://doi.org/10.33619/2414-2948/79/48
30. Lee S.H., Lee D.W., Lee S.H., Park C.K., Lim K.J., Shin W.S. Contact resistivity and adhesion of copper alloy seed layer for copper-plated silicon heterojunction solar cells. *Japanese Journal of Applied Physics*. 2018; 57(8S3): 08RB13. https://doi.org/10.7567/JJAP.57.08RB13
31. Gheidari M., Soleimani E.A. A study of Al/Ti, Al/Ni/Cr AND Al/Mo ohmic contacts to indium tin oxide (ITO) for application in thin film solar cell. In: Goswami D.Y., Zhao Y. (eds.) *Proceedings of ISES World Congress 2007* (Vols. I–V). Berlin, Heidelberg: Springer; 2007: 1123–1125. https://doi.org/10.1007/978-3-540-75997-3_221